J|A|C|S
ARTICLES
Published on Web 02/14/2003

Structural Model for an Alkaline Form of Ferricytochrome *c*

Michael Assfalg,[†] Ivano Bertini,*[,†] Alessandra Dolfi,[†] Paola Turano,[†] A. Grant Mauk,[‡] Federico I. Rosell,[‡] and Harry B. Gray[§]

Contribution from the CERM, University of Florence, Via Luigi Sacconi 6, 50019 Sesto Fiorentino, Florence, Italy, Department of Biochemistry and Molecular Biology, University of British Columbia, Vancouver, British Columbia V6T 1Z3, Canada, and Beckman Institute, California Institute of Technology, Pasadena, California 91125

Received June 5, 2002; E-mail: bertini@cerm.unifi.it

Abstract: An ^{15}N-enriched sample of the yeast *iso*-1-ferricytochrome *c* triple variant (Lys72Ala/Lys79Ala/Cys102Thr) in an alkaline conformation was examined by NMR spectroscopy. The mutations were planned to produce a cytochrome *c* with a single conformer. Despite suboptimal conditions for the collection of spectra (i.e., pH $\approx$ 11), NMR remains a suitable investigation technique capable of taking advantage of paramagnetism. 76% of amino acids and 49% of protons were assigned successfully. The assignment was in part achieved through standard methods, in part through the identification of groups maintaining the same conformation as in the native protein at pH 7 and, for a few other residues, through a tentative analysis of internuclear distance predictions. Lys73 was assigned as the axial ligand together with His18. In this manner, 838 meaningful NOEs for 108 amino acids, 50 backbone angle constraints, and 203 pseudocontact shifts permitted the convergence of randomly generated structures to a family of conformers with a backbone RMSD of 1.5 $\pm$ 0.2 Å. Most of the native cytochrome *c* conformation is maintained at high pH. The NOE pattern that involves His18 clearly indicates that the proximal side of the protein, including the 20s and 40s loops, remains essentially intact. Structural differences are concentrated in the 70−80 loop, because of the replacement of Met80 by Lys73 as an axial ligand, and in the 50s helix facing that loop; as a consequence, there is increased exposure of the heme group to solvent. Based on several spectral features, we conclude that the folded polypeptide is highly fluxional.

Introduction

The influence of pH on mitochondrial ferricytochrome *c* was first recognized over 60 years ago.[1−5] In the pH range 1−12, at least five distinct forms of the protein can be detected that are now known to result from altered protein folding and heme iron axial coordination.[6] Of these conformations, the native state is the dominant form near neutral pH, and the structures of the reduced and oxidized forms of the native conformer have been studied extensively at near-atomic resolution by both X-ray crystallography[7−13] and NMR spectroscopy.[14−18] By comparison, no structural data are yet available for the so-called alkaline conformers, which form with pK_a's in the 8.5−10.5 range, depending on the species from which the cytochrome originates and the solution conditions.[19−22] Although spectroscopic evidence indicates that Met80 is replaced by Lys73 or Lys79 (or Lys72 in some cases) as an axial heme iron ligand,[23−25] and although structural models have been calculated based on this information,[26] definitive structural characterization of any one of the alkaline ferricytochrome *c* conformers is lacking.

[†] University of Florence.
[‡] University of British Columbia.
[§] California Institute of Technology.

(1) Theorell, H. *Biochem. Z.* **1936**, *285*, 207−218.
(2) Theorell, H.; Akesson, A. *J. Am. Chem. Soc.* **1941**, *63*, 1804−1811.
(3) Theorell, H.; Akesson, A. *J. Am. Chem. Soc.* **1941**, *63*, 1812−1814.
(4) Theorell, H.; Akesson, A. *J. Am. Chem. Soc.* **1941**, *63*, 1815−1820.
(5) Theorell, H. *J. Am. Chem. Soc.* **1941**, *63*, 1820−1827.
(6) Wilson, M. T.; Greenwood, C. In *Cytochrome c. A multidisciplinary approach*; Scott, R. A., Mauk, A. G., Eds.; University Science Books: Sausalito, CA, 1996; pp 611−634.
(7) Louie, G. V.; Brayer, G. D. *J. Mol. Biol.* **1990**, *214*, 527−555.
(8) Bushnell, G. W.; Louie, G. V.; Brayer, G. D. *J. Mol. Biol.* **1990**, *214*, 585−595.
(9) Berghuis, A. M.; Brayer, G. D. *J. Mol. Biol.* **1992**, *223*, 959−976.
(10) Murphy, M. E. P.; Nall, B. T.; Brayer, G. D. *J. Mol. Biol.* **1992**, *227*, 160−176.
(11) Takano, T.; Dickerson, R. E. *J. Mol. Biol.* **1981**, *153*, 79−94.
(12) Takano, T.; Dickerson, R. E. *J. Mol. Biol.* **1981**, *153*, 95−155.
(13) Ochi, H.; Hata, Y.; Tanaka, N.; Kakudo, M.; Sakuri, T.; Achara, S.; Morita, Y. *J. Mol. Biol.* **1983**, *166*, 407−418.
(14) Baistrocchi, P.; Banci, L.; Bertini, I.; Turano, P.; Bren, K. L.; Gray, H. B. *Biochemistry* **1996**, *35*, 13788−13796.
(15) Banci, L.; Bertini, I.; Bren, K. L.; Gray, H. B.; Sompornpisut, P.; Turano, P. *Biochemistry* **1997**, *36*, 8992−9001.
(16) Banci, L.; Bertini, I.; Gray, H. B.; Luchinat, C.; Reddig, T.; Rosato, A.; Turano, P. *Biochemistry* **1997**, *36*, 9867−9877.
(17) Banci, L.; Bertini, I.; Huber, J. G.; Spyroulias, G. A.; Turano, P. *JBIC, J. Biol. Inorg. Chem.* **1999**, *4*, 21−31.
(18) Qi, P. X.; Beckman, R. A.; Wand, A. J. *Biochemistry* **1996**, *35*, 12275−12286.
(19) Osheroff, N.; Borden, D.; Koppenol, W. H.; Margoliash, E. *J. Biol. Chem.* **1980**, *255*, 1689−1697.
(20) Moore, G. R.; Pettigrew, G. W. *Cytochromes c; Evolutionary, Structural and Physicochemical Aspects*; Springer-Verlag: Berlin, 1990.
(21) Pettigrew, G. W.; Moore, G. R. *Cytochromes c; Biological Aspects*; Springer-Verlag: Berlin, 1987.
(22) Pearce, L. L.; Gärtner, A. L.; Smith, M.; Mauk, A. G. *Biochemistry* **1989**, *28*, 3152−3156.
(23) Rosell, F. I.; Ferrer, J. C.; Mauk, A. G. *J. Am. Chem. Soc.* **1998**, *120*, 11234−11245.
(24) Ferrer, J. C.; Guillemette, J. G.; Bogumil, R.; Inglis, S. C.; Smith, M.; Mauk, A. G. *J. Am. Chem. Soc.* **1993**, *115*, 7507−7508.
(25) Pollock, W. B. R.; Rosell, F. I.; Twitchett, M. B.; Dumont, M. E.; Mauk, A. G. *Biochemistry* **1998**, *37*, 6124−6131. N.B. Cytochrome *c* expressed in yeast is normally trimethylated at Lys72.

Structural characterization of the alkaline ferricytochrome *c* conformers is an essential step toward an understanding of the linkage of cytochrome *c* conformation to both the pH and oxidation state of the heme iron. While the structure of ferricytochrome exhibits at least five pH-linked conformational states, ferrocytochrome exhibits only three (that form with pK_a's of 2.5 and 12). Consequently, reduction of alkaline ferricytochrome *c* at moderately alkaline pH results in prompt formation of the native ferrocytochrome. The transient stability of alkaline ferrocytochrome conformer demonstrates the profound functional dependence of the protein on pH. The structural basis for the greatly lowered reduction potential of the alkaline conformer,[27] however, remains speculative.

While the biological consequences of the alkaline conformational transition of ferricytochrome *c* have been discounted by some authors,[6] this issue is open to debate. For example, resonance Raman spectroscopy[28] provides evidence that binding of ferricytochrome *c* to cytochrome *c* oxidase induces dissociation of Met80 from the heme iron of the ferricytochrome, an event that is required for formation of the alkaline conformers. As the midpoint reduction potential of alkaline cytochrome *c* is substantially lower than that of the native protein, the alkaline isomerization or displacement of the Met80 ligand upon formation of this complex may constitute a conformational gate to ensure unidirectional electron transfer between two heme centers that otherwise have nearly equivalent potentials. In addition, the alkaline conformers may be regarded as intermediate states in the unfolding of the ferricytochrome under conditions that are often used to probe these processes. Both chemical denaturants and elevated temperatures decrease the apparent pK_a for alkaline isomerization(s) and thereby influence the mechanism of re/unfolding.[29,30] As a result, it is conceivable that one or more alkaline-like species may be involved in the folding pathway(s) of cytochrome *c* under native conditions.

The present study represents an essential first step toward full structural characterization of alkaline ferricytochrome *c* by focusing on the structure of the conformer in which Lys73 is believed to coordinate to the heme iron. This conformer, which is one of the two roughly equally populated alkaline forms of native cyt *c*,[23] was selected because inspection of the structure of the native ferricytochrome and modeling studies[26] indicate that this conformer should differ the most from that of the native protein.

Determination of the solution structure characterization of this protein form at high pH required a nonstandard approach involving extensive use of paramagnetic-based constraints.

Materials and Methods

Protein Preparation. The yeast *iso*-1-cytochrome *c* triple variant Lys72Ala/Lys79Ala/Cys102Thr was expressed in *E. coli* containing the phagemid pBTR as described elsewhere.[25] The lysyl residues at positions 72 and 79 were replaced with alanine to ensure that only one alkaline conformer forms at elevated pH.[24,25] Cys102 was replaced with threonine to avoid protein autoreduction and to preclude protein dimerization. This triple variant is referred to in this report as K79A. ^{15}N-enriched protein was expressed essentially as described by Morar et al.[31]

NMR Spectroscopy. NMR samples were prepared by diluting a concentrated stock of protein to a concentration of ~2 mM in 50 mM sodium phosphate buffer, pH 7.0. NaOH was added to raise the pH as necessary.

All NMR data were acquired at 298 K on Bruker Avance spectrometers operating at proton Larmor frequencies of 700.13 and 800.13 MHz.

^{1}H 1D data (800 MHz) were recorded on a spectral window of 80 ppm. Suppression of the intense water signal was obtained by presaturation.

^{1}H−^{15}N HSQC spectra[32] (800 MHz) were acquired on H_2O samples at pH values in the range 7.0−11.1. 3D TOCSY-^{15}N HSQC and NOESY-^{15}N HSQC spectra[33,34] were recorded at 800 MHz in H_2O solution with 1024(^{1}H) × 100(^{15}N) × 512(^{1}H) data points. In these experiments, the delay between the ^{1}H 90° pulse following the mixing time period and the first subsequent ^{15}N 90° pulse was set to 5.5 ms ($\approx 1/2J_{NH}$), the mixing time was 100 ms. Spectral windows of 32, 10, and 12 ppm were used, respectively, for ^{15}N, direct ^{1}H dimension, and indirect ^{1}H dimension. Quadrature detection was performed in the TPPI mode for F1 and in the echo−antiecho/TPPI mode for F2. The latter mode allowed also for water signal suppression.

Axial ligand protons have been identified by ^{1}H nuclear Overhauser effect (NOE) experiments (at 700 MHz) performed using a super WEFT pulse sequence for the suppression of slow relaxing nuclei resonances and collected as previously reported.[35]

Further dipolar connectivities have been revealed by two-dimensional NOESY experiments. TPPI NOESY spectra[36,37] (800 MHz) were recorded with presaturation of the solvent signal during both the relaxation delay and the mixing time. To optimize the detection of cross peaks involving fast-relaxing resonances, NOESY maps were recorded on the full spectral width (80 ppm) with a recycle time of 300 ms and a mixing time of 50 ms. To optimize the detection of connectivities in the diamagnetic region, NOESY maps were recorded on a smaller spectral width (32 ppm) with a recycle time of 800 ms and a mixing time of 100 ms. Analogously, a TPPI TOCSY experiment[38] was performed with presaturation during the relaxation delay on a spectral width of 32 ppm (recycle time of 800 ms and spin lock time of 100 ms). For all the 2D maps, 1024 experiments were done with 2048 data points in the F2 direction. The data were multiplied in both dimensions by a pure cosine-squared bell window function and Fourier transformed to obtain 2048 × 2048 real data points.

Analysis of the Spectra. Data processing was performed with a Silicon Graphics workstation and the Bruker software package. The 2D and 3D maps were analyzed with the aid of the program XEASY.[39] Of the 3D TOCSY-^{15}N HSQC and NOESY-^{15}N HSQC experiments performed at several pH values in the range 9−11, the spectra collected at pH 11 were selected for peak analysis, as the others were all complicated by a severe overlap of resonances with those of the native protein. Connectivities identified by 1D NOEs were all converted into upper distance limits of 5.0 Å. The volumes of the NOESY cross peaks between assigned resonances were integrated manually with an elliptical

(26) Ness, S. R.; Lo, T. P.; Mauk, A. G. *Isr. J. Chem.* **2000**, *40*, 21−25.
(27) Barker, P. B.; Mauk, A. G. *J. Am. Chem. Soc.* **1992**, *114*, 3619−3624.
(28) Döpner, S.; Hildebrandt, P.; Rosell, F. I.; Mauk, A. G.; Soulimane, T.; Bouse, G. *Eur. J. Biochem.* **1999**, *261*, 379−391.
(29) Banci, L.; Bertini, I.; Spyroulias, G. A.; Turano, P. *Eur. J. Inorg. Chem.* **1998**, *1*, 583−591.
(30) Russell, B. S.; Melenkivitz, R.; Bren, K. L. *Proc. Natl. Acad. Sci. U.S.A.* **2000**, *97*, 8312−8317.
(31) Morar, A. S.; Kakouras, D. S.; Young, G. B.; Boyd, J.; Pielak, G. *JBIC, J. Biol. Inorg. Chem.* **1999**, *4*, 220−222.
(32) Davis, L. A.; Keller, J.; Laue, E. D.; Moskau, D. *J. Magn. Reson.* **1992**, *98*, 207−216.
(33) Kay, L. E.; Marion, D.; Bax, A. *J. Magn. Reson.* **1989**, *84*, 72−84.
(34) Marion, D.; Kay, L. E.; Sparks, S. W.; Torchia, D. A.; Bax, A. *J. Am. Chem. Soc.* **1989**, *111*, 1515−1517.
(35) Banci, L.; Bertini, I.; Luchinat, C.; Piccioli, M.; Scozzafava, A.; Turano, P. *Inorg. Chem.* **1989**, *28*, 4650−4656.
(36) Macura, S.; Wüthrich, K.; Ernst, R. R. *J. Magn. Reson.* **1982**, *47*, 351−357.
(37) Marion, D.; Wüthrich, K. *Biochem. Biophys. Res. Commun.* **1983**, *113*, 967−974.
(38) Bax, A.; Davis, D. G. *J. Magn. Reson.* **1985**, *65*, 355−360.
(39) Bartels, C.; Xia, T. H.; Billeter, M.; Güntert, P.; Wüthrich, K. *J. Biomol. NMR* **1995**, *5*, 1−10.

integration routine. The intensities of these features were converted into upper limits of interatomic distances by following the methodology of the program CALIBA.[40] NOE-based angle constraints can be obtained for the helical fragments in a protein;[41] the occurrence of $d_{N\alpha}(i,i)NOE/d_{\alpha N}(i-1,i)NOE < 1$ for amino acids 10, 11, 13, 53, 54, 63−69, and 91−100 confirms their helicoidal conformation. Therefore, ψ and ϕ angle constraints were imposed to better define the backbone conformation of these segments during the calculation.

Pseudocontact Shift Constraints and Determination of the Paramagnetic Susceptibility Anisotropy. Pseudocontact shifts arise from the magnetic susceptibility anisotropy and depend on the nuclear position with respect to the principal axes of the magnetic susceptibility tensor. Within the metal-centered point-dipole/point-dipole approximation, the following equation holds:[42,43]

$$\delta_i^{pc} = \frac{1}{12\pi r_i^3}\left[\Delta\chi_{ax}^{para}(3n_i^2 - 1) + \frac{3}{2}\Delta\chi_{rh}^{para}(l_i^2 - m_i^2)\right] \quad (1)$$

where $\Delta\chi^{para}_{ax}$ and $\Delta\chi^{para}_{rh}$ are the axial and rhombic anisotropies of the magnetic susceptibility tensor, l_i, m_i, and n_i are the direction cosines of the position vector of atom i with respect to the magnetic susceptibility tensor coordinate system, and r_i is the distance between the paramagnetic center and the proton i.

According to eq 1, pseudocontact shifts contain structural information and can be used as structural constraints.[44,45] These are long range constraints in that they decrease with the reciprocal of the third power of the metal-nucleus distance. As a result, pseudocontact shifts fix the reciprocal position of protein protons and the metal center.

The pseudocontact shift values were estimated by subtracting the chemical shifts measured for the totally reduced, diamagnetic, native form of the protein[14] from the corresponding shifts of the completely oxidized, paramagnetic form of the K79A cytochrome variant at pH 11.1. It is reasonably assumed that there is no large difference in the corresponding diamagnetic shift of the two proteins (vide infra). In any case, a larger tolerance (0.8 ppm) was given to the constraints of the residues in the 70−80 loop. Only those protons for which no contact contribution to the hyperfine shift was expected were considered. The resonances of protons of the two heme-bound cysteines, histidine, and lysine axial ligands of the heme and heme moiety were, therefore, not included in the calculations. Also the resonances of diastereotopic groups were not included.

The five independent magnetic susceptibility anisotropy tensor parameters ($\Delta\chi_{ax}^{para}$, $\Delta\chi_{rh}^{para}$, and three independent direction cosines that define the principal directions of the χ^{para} tensor with respect to the chosen axis system) were evaluated by best fitting an extended set of equations like eq 1, with the position vectors for each proton obtained from the starting structure, to the same set of experimental pseudocontact shift values. This calculation was performed with the program FANTASIAN (available at www.postgenomicnmr.net).[46] Monte Carlo methods were used to make error estimates for all tensor parameters: 200 different calculations were performed on data sets, where 30% of experimental values were randomly eliminated from input data.

Generation of a Family of Structures. A family of structures was generated starting from random conformations through the PARAMAGNETIC-DYANA program (available at www.postgenomicnmr.net).[47] The heme cofactor was introduced into the structure calculations as described previously.[16] The coordination bond with the axial ligands was introduced using upper and lower distance limits between the iron and the donor atoms. 500 random structures were annealed in 10 000 steps under the effect of the final set of NMR constraints. The PARAMAGNETIC-DYANA calculations including pcs were performed both by fixing the origin of the magnetic susceptibility tensor on the iron atom and by allowing the pseudoresidue representing the tensor to find the best position for the origin under the effect of the experimental constraints only. The fact that with the latter procedure the origin of the tensor was still coincident with the iron atom shows that the five tensor parameters represent a well-defined solution. The final family of structures with the lowest target function was energy-minimized with the program AMBER 6.0[48] imposing the same set of experimental constraints used in PARAMAGNETIC-DYANA.

Structure Analysis. The quality of the final structures has been analyzed in terms of ideal geometry parameters with the program PROCHECK.[49] The dipolar connectivities expected on the basis of the final structure have been back-calculated with the program CORMA.[50] The degree of agreement between experimental and back-calculated constraints was taken as a further evaluation criterion of the accuracy of the structure. Solvent accessibility was evaluated with the program MOLMOL.[51]

Results and Discussion

Analysis of the Alkaline Transition of Ferricytochrome *c* by NMR Spectroscopy. The 1D ^{1}H NMR spectrum of the native K79A cytochrome *c* variant at pH 7 indicates that the electronic structure of the metal center, and thus the conformation of the ligands and of the nearby residues, is substantially unchanged with respect to the native protein (Figure 1).

Also the ^{1}H−^{15}N HSQC spectra of the variant and wild-type proteins[31,52] do not show significant differences in the shifts of both the proton and nitrogen resonances of the backbone amidic groups (Figure 2). The same holds true for the side chains of Trp59, the asparagines, and the glutamines. Thus, no significant changes occur in the conformation of the backbone and the side chains of these residues upon mutation, as expected on the basis of the location of the three mutated residues.

The alkaline transition can be followed by NMR spectroscopy.[23,24,53] With increasing pH, new resonances appear in the 1D ^{1}H NMR spectrum of the K79A cytochrome variant (Figure 3) at 26.6, 25.9, 24.5, 19.5, 17.2, 15.4, and −10.3 ppm. At the same time, the hyperfine-shifted signals of the native form decrease in intensity and then disappear. Among these signals are those corresponding to the side chain of Met80 (−30.2 (γ) and −22.4 (ϵ) ppm), which is bound to the iron at neutral pH. Because two distinct sets of resonances are observable at intermediate pH, the exchange between the neutral and the alkaline form of the protein is slow on the NMR time scale. The chemical shift values of the alkaline heme methyl reso-

(40) Güntert, P.; Braun, W.; Wüthrich, K. *J. Mol. Biol.* **1991**, *217*, 517−530.
(41) Gagne′, R. R.; Tsuda, S.; Li, M. X.; Chandra, M.; Smillie, L. B.; Sykes, B. D. *Protein Sci.* **1994**, *3*, 1961−1974.
(42) Bertini, I.; Luchinat, C.; Parigi, G. *Solution NMR of Paramagnetic Molecules*; Elsevier: Amsterdam, 2001.
(43) Bertini, I.; Luchinat, C. *NMR of paramagnetic molecules in biological systems*; Benjamin/Cummings: Menlo Park, CA, 1986.
(44) Banci, L.; Bertini, I.; Cremonini, M. A.; Gori Savellini, G.; Luchinat, C.; Wüthrich, K.; Güntert, P. *J. Biomol. NMR* **1998**, *12*, 553−557.
(45) Banci, L.; Bertini, I.; Gori Savellini, G.; Romagnoli, A.; Turano, P.; Cremonini, M. A.; Luchinat, C.; Gray, H. B. *Proteins Struct. Funct. Genet.* **1997**, *29*, 68−76.
(46) Banci, L.; Bertini, I.; Bren, K. L.; Cremonini, M. A.; Gray, H. B.; Luchinat, C.; Turano, P. *JBIC, J. Biol. Inorg. Chem.* **1996**, *1*, 117−126.
(47) Barbieri, R.; Bertini, I.; Cavallaro, G.; Lee, Y. M.; Luchinat, C.; Rosato, A. *J. Am. Chem. Soc.* **2002**, *124*, 5581−5587.
(48) Case, D. A.; Pearlman, D. A.; Caldwell, J. W.; Cheatham, T. E.; Ross, W. S.; Simmerling, C. L.; Darden, T. A.; Merz, K. M.; Stanton, R. V.; Cheng, A. L.; Vincent, J. J.; Crowley, M.; Tsui, V.; Radmer, R. J.; Duan, Y.; Pitera, J.; Massova, I.; Seibel, G. L.; Singh, U. C.; Weiner, P. K.; Kollman, P. A. *AMBER 6*; University of California: San Francisco, CA, 1999.
(49) Laskowski, R. A.; Rullmann, J. A. C.; MacArthur, M. W.; Kaptein, R.; Thornton, J. M. *J. Biomol. NMR* **1996**, *8*, 477−486.
(50) Borgias, B.; Thomas, P. D.; James, T. L. COmplete Relaxation Matrix Analysis (CORMA), 5.0 ed.; University of California: San Francisco, CA, 1989 (GENERIC). Ref Type: Computer Program.
(51) Koradi, R.; Billeter, M.; Wüthrich, K. *J. Mol. Graphics* **1996**, *14*, 51−55.
(52) Fetrow, J. S.; Baxter, S. M. *Biochemistry* **1999**, *38*, 4480−4492.
(53) Hong, X.; Dixon, D. W. *FEBS Lett.* **1989**, *246*, 105−108.

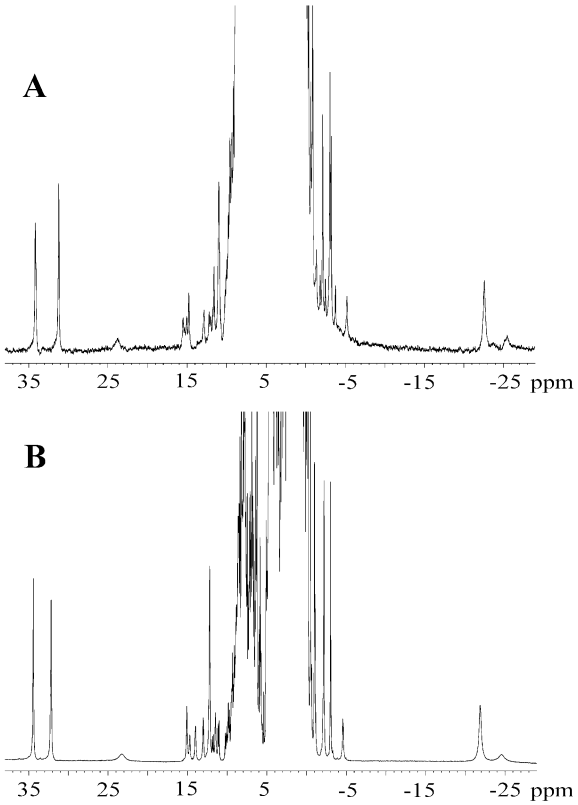

Figure 1. ^{1}H NMR spectra of the native (A) oxidized wild-type and (B) K79A cytochrome *c* (50 mM phosphate buffer, pH 7, and 298 K).

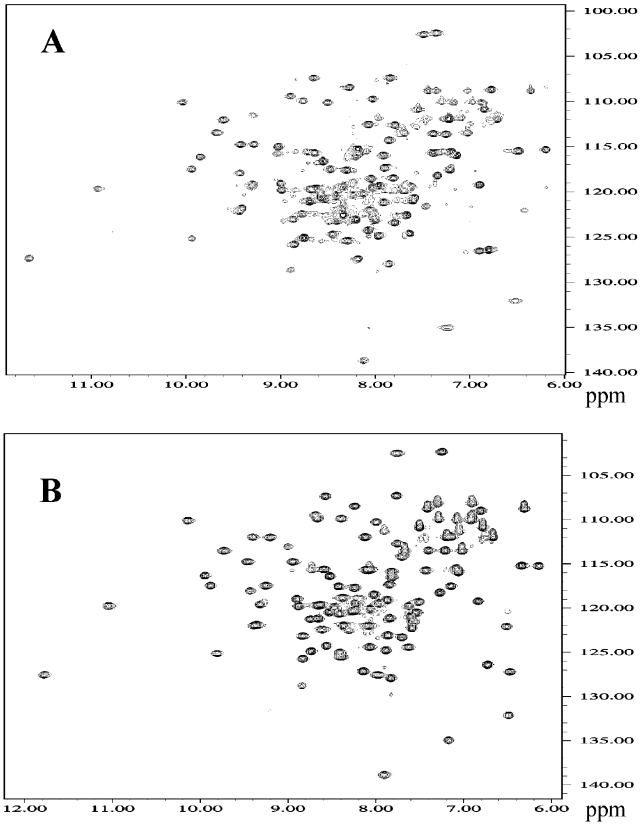

Figure 2. ^{1}H−^{15}N-HSQC NMR spectra of the native (A) oxidized wild-type and (B) the K79A cytochrome *c* variant (50 mM phosphate buffer, pH 7, and 298 K).

nances are similar to those observed for the cyanide adduct of the M80A cytochrome variant and the NH_3 adduct of wild-type ferricytochrome *c*[29,54] (Table 1). At high pH, the spectrum also closely resembles that of ferricytochrome *c* recorded at high temperature[29] or in the presence of denaturing agents[30] (data not shown). The analogy between the spectrum of the K79A cytochrome variant at high pH and the spectra of the previously mentioned adducts suggests that a new ligand replaces Met80 under these conditions and that this new ligand does not contribute to the rhombicity of the magnetic anisotropy tensor. The present work reports the first observation of signals attributable to the sixth ligand to the iron in the alkaline conformer of the K79A cytochrome variant obtained at pH 11.1. These broad and shifted signals are emphasized with an asterisk in Figure 3.

The alkaline transition is also evident in ^{1}H−^{15}N HSQC spectra (Figure 4). In this case, it appears that slow exchange occurs, as indicated by the appearance of new resonances that increase in intensity as the pH increases. At pH 11.1, the signals of 94 backbone NHs, the side chains of three Gln/Asn, and the NH of Trp59 are still detectable, although their intensity is reduced with respect to that at pH 7. The large number of detectable NH resonances at this very high pH can be taken as an indication of a high level of protection for these NHs and is, therefore, consistent with a globular structure of the alkaline form of the protein. The chemical shift dispersion of the new species is comparable to that of the native protein, indicating that this species is characterized by a well-defined three-dimensional structure. From the differences in chemical shifts

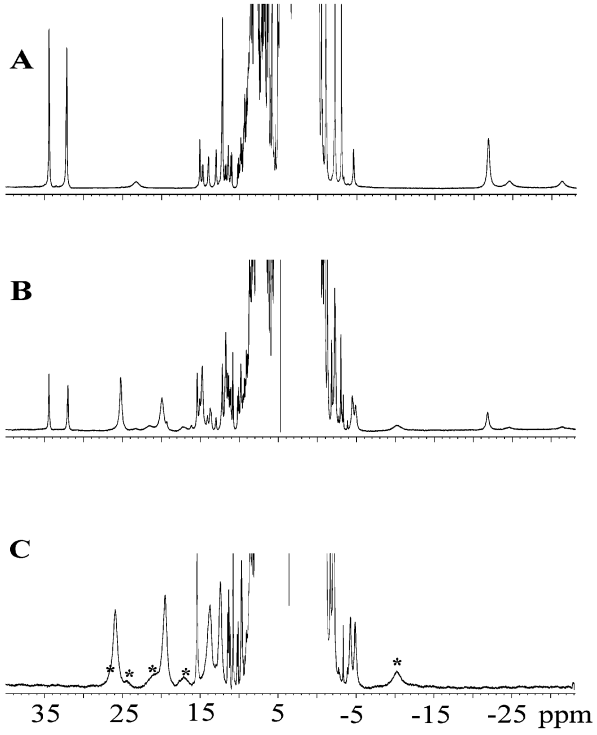

Figure 3. ^{1}H NMR spectra of the K79A cytochrome *c* variant recorded at (A) pH 7.1, (B) pH 9.7, and (C) pH 11.1 (298 K). Broad signals attributed to the axial ligands to the iron are marked with an *.

observed for corresponding signals in the native and alkaline states of the protein, a correlation time for the exchange process can be estimated to be $\tau_M \gg 1$ ms. Unfortunately, the exchange

(54) Bren, K. L.; Gray, H. B.; Banci, L.; Bertini, I.; Turano, P. *J. Am. Chem. Soc.* **1995**, *117*, 8067−8073.

Table 1. Chemical Shift Values (ppm) of the Heme Methyl Resonances of the Alkaline Form of Yeast Ferricytochrome *c* K79A, the Native Yeast Ferricytochrome *c*,[15] the Cyanide Adduct of Yeast Ferricytochrome *c* M80A,[46] the High Temperature Form of Horse Heart Ferricytochrome *c* (three species),[16] and the NH_3 Adduct of Horse Heart Cytochrome *c*[29]

assignment	alkaline K79A yeast cytochrome *c* (298 K)	wild-type yeast cytochrome *c* (303 K)	M80A yeast cytochrome *c*-CN^- (303 K)	horse heart cytochrome *c* (335 K)	horse heart cytochrome *c*-NH_3 (293 K)
8-CH_3	25.6	34.7	22.5	22.3 22.0 20.7	25.2
3-CH_3	12.1	31.0	11.3	12.4 13.6 11.3	11.0
5-CH_3	19.5	11.0	19.5	20.6 18.9 20.2	23.5
1-CH_3	14.2	8.0	15.4	12.7 12.4 13.4	15.5

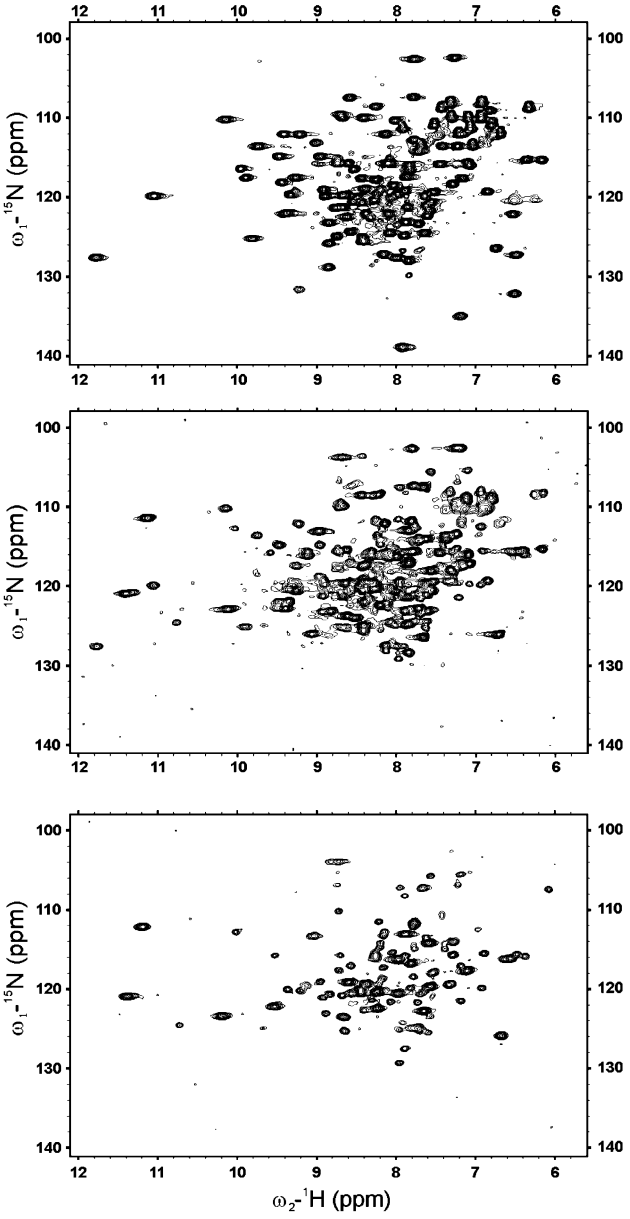

Figure 4. $^1H-^{15}N$-HSQC NMR spectra of the K79A cytochrome *c* variant recorded at (A) pH 7.1, (B) pH 9.7, and (C) pH 11.1 (298 K).

rate is too slow to allow the assignment of the new signals through saturation transfer experiments.

Sequence-Specific Assignment. Structural characterization of the alkaline isomers of ferricytochrome *c* in solution proved to be a highly challenging task. Typically, the procedure to determine the structure of a ^{15}N-labeled protein of comparable size begins with the sequence-specific assignment of individual amino acid resonances. Amino acid spin patterns are identified by TOCSY-type experiments, and connectivities between adjacent residues are then established based on sequential and medium range NOEs. With a similar approach, solution structures of the neutral conformer of cytochrome *c* in both oxidation states have been elucidated.[14,15] At the elevated pH required to convert the present protein completely to its alkaline conformer (pH > 11 under the experimental conditions required for NMR spectroscopy), most of the backbone NHs are still detectable, although with reduced intensity. Furthermore, this system is characterized by a low number of detectable NOESY cross peaks as it happens in the presence of extensive sub-nanosecond mobility. This finding is consistent with the intensities of the $\{^1H\}-^{15}N$ heteronuclear NOEs of the alkaline species (unpublished work), which indicate a local reorientational correlation time shorter than the rotational correlation time.

Chemical shifts of residues Gln16, His18, Thr19, Gly29, Asn31, and Leu32 were identified easily because their spin patterns are resolved outside the diamagnetic envelope. The sequence-specific assignment was then extended through the analysis of the $^1H-^{15}N$ NOESY and TOCSY spectra using the standard approach. This approach allowed the assignment of residues 9−19, 29−46, 52−60, 62−70, and 90−103. The identification of the resonances of these residues was helpful for the assignment of heme signals. The signals of the four methyl groups of the heme are well resolved at 25.6, 19.6, 14.2, and 12.1 ppm. The resonances at 25.6 and 14.2 ppm display a strong dipolar connectivity to a signal at −4.9 ppm. The only proton which is equidistant from two methyl groups is the *δ-meso*, positioned between the 1-CH_3 and the 8-CH_3 groups. The signal at 14.2 ppm can be assigned to 1-CH_3 because it has a connectivity with the signals of a thioether group. The assignment of the signal at 25.6 ppm as 8-CH_3 is consistent with its connectivities with δ-CH_3 of Leu32 and ϵ-CH_3 of Met64. The remaining resonances are assigned to methyls 3 and 5. The resonance at 19.6 ppm is assigned to 5-CH_3 due to its connectivities to Gly29 and Pro30. The resonances of the other heme substituents are assigned by analyzing the NOESY

connectivities, starting from position 1 and 3 and "hopping" around the macrocycle. The previously described NOE patterns observed between heme resonances and amino acid side chains indicate that the relative position of these residues and the cofactor are substantially maintained in the alkaline species. Under this assumption and on the basis of NOE connectivities between the heme thioether-2 and an aromatic ring, the Phe82 could be identified.

The 1D NMR spectra show very broad signals, which do not exchange in D_2O solution and that resonate at 26.6, 24.5, 21.0, 17.2, and −10.2 ppm. The line widths of these signals suggest that they are due to protons of the metal ligands, most probably the axial ligands. The saturation of the signal at −10.2 ppm allows the detection of an NOE with a proton resonating at 13.8 ppm, which displays a NOESY connectivity to a Hβ proton of His18. This NOE pattern is consistent with the assignment of the broad signal to Hϵ1 and the signal at 13.8 ppm to Hδ1 of His18. The detectability of the side chain Hδ1 of His18 at pH 11.1 indicates that its H-bond with Pro30 is preserved. By saturation of the signal at 21.0 ppm, an NOE peak is observed for the backbone NH and the other Hβ of His18. Therefore, the saturated signal is assigned to Hδ2 of His18. With the signals of His18 completely assigned, the remaining broad signals at 26.6, 24.5, and 17.2 ppm should arise from the sixth ligand to the iron. Saturation of these three signals does not give rise to NOEs to protons of known assignment. However, NOEs are detectable between the signal at 24.5 ppm and unidentified signals resonating at 10.9 and 9.4 ppm. The latter two resonances have NOE connectivities to known resonances, which allow us to locate them close to the β-CH_2 protons of Phe82 and to the Hα proton of heme thioether-2. This result is a further indication that the broad resonances are due to the sixth ligand. In the present protein, the only reasonable ligand among the unassigned amino acids is Lys73, in accordance with previous results.[23,30] The detection of this resonance is by itself an important achievement. Unfortunately, no scalar connectivities could be detected for any of these signals that would have allowed the obtainment of a proton-specific assignment of the side chain signals. Thus, the assignment was made, based on the relative line widths of the resonances, on the observed NOE patterns and on their comparison to our preliminary structural model. Based on their line widths and chemical shifts, we propose that the three signals at 26.6, 24.5, and 17.2 ppm are due to the Lys73 side chain Hϵ's and Hδ's (i.e., to those protons that will be closer to the iron upon binding). The two sharper resonances at 10.9, and 9.4 ppm are assigned to the Hβ's of Lys73, based on their NOESY cross-peaks to Phe82 and heme thioether-2. The presence of NOEs between these sharp resonances and the broad signal at 24.5 ppm suggests that the broad signal is one of the Hδ's. An additional signal at 6.7 ppm has NOESY connectivities to Lys73 Hβ's and to the Hα proton of heme thioether-2 and can be attributed tentatively to one of the Hγ's of Lys73. Given the NOESY connectivities to the nearby Phe82 and the Hα proton of heme thioether-2, the backbone NH of Ala72 was also identified. NOEs with this resonance allowed the assignment of the HN and Hα of Lys73 and the Hα of Pro71. The complete set of connectivities described previously is summarized in Chart 1, where the chemical shifts of some of the hyperfine-shifted resonances are also reported.

Chart 1. NOE Patterns Involving the Heme and Its Axial Ligands

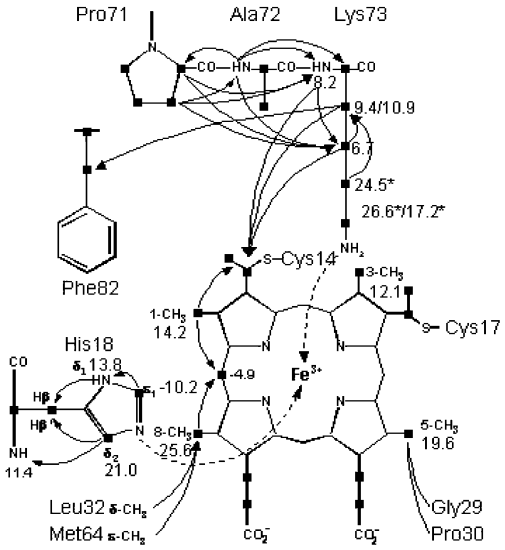

Further residues could be assigned in an iterative process which involves the calculation of a model structure, back-calculation of the expected NOEs, and comparison with the experimental data. This procedure led to the identification of Phe-3, Lys-2, Gly24, Tyr48, Thr49, and residues 83−87. This approach is based on an intensive and recursive use of the program CORMA, which uses a relaxation matrix approach to calculate expected NOEs for a given structure. The reference structure was generated through preliminary structure calculations obtained by imposing Lys73 binding. Spin patterns for residues −3, 24, 48, and 84−87 have been identified a posteriori in TOCSY-type experiments, thus confirming the nature of those amino acids. For residues −2, 49, and 83, the assignment is based only on the presence of typical dipolar connectivities with other residues.

The architecture of the protein in the 74−81 loop should change significantly at high pH to accommodate the ligand exchange. The starting point for the assignment of residues in this protein fragment relies on the identification of the spin pattern of an Ile residue with NOE connectivities with residues spatially close in the structure, that is, 55, 57, 58, 59, 60, 63, and 68. The only unidentified Ile at this stage is Ile75, but the assignment of the previously described pattern to Ile75 implies a major rearrangement of the structure of this area. Furthermore, residues 79−81 have been identified by the unique sequence pattern Ala-Met-Ala and by the observation of NOE cross peaks Ala81-Gly83, Ala81-Gly84, and Met80-Gly84 to support the assignment of the entire loop.

All assignments are reported in Table 1 of the Supporting Information. Of the expected ^{1}H resonances, 49% of the signals due to NHs and nonexchangeable protons have been assigned, plus 10 resonances corresponding to exchangeable side-chain protons. Resonances for 82 amino acid residues have been identified, which correspond to 76% of the total sequence. The only unassigned protein fragments longer than three amino acids are within the *N*-terminus and the 20s loop. It is noteworthy that both of these regions are also ill-defined in the structure of the native protein.

The long range NOEs needed for structural calculations were obtained through an extensive use of the program CORMA, as

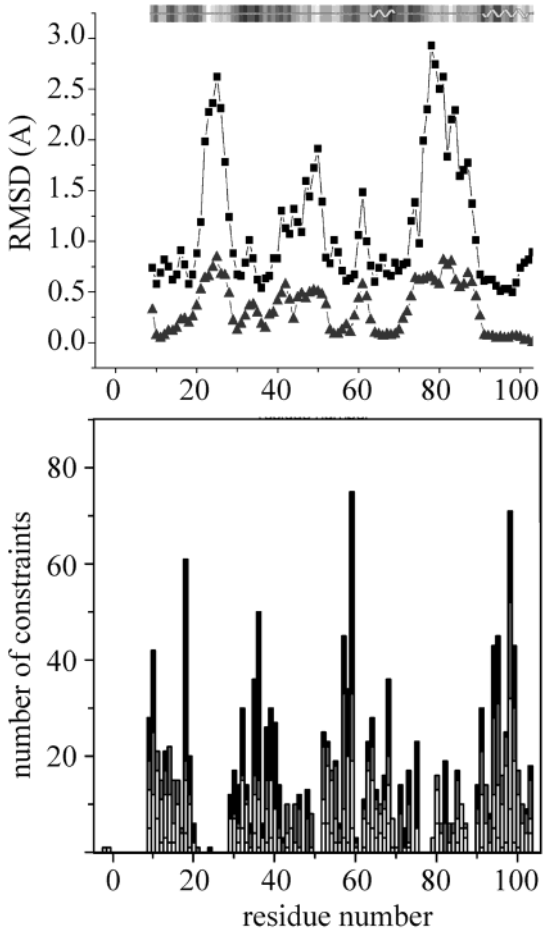

Figure 5. The number of experimental NOEs per residue is correlated with the global (■) and local (▲) backbone RMSD per residue calculated from the 20 structures of the REM family with respect to the averaged structure. Black, dark gray, light gray, and white bars represent long, medium, sequential, and intraresidue NOEs, respectively. (Top panel, inset) The secondary structure elements of the averaged structure determined with the program Procheck-NMR are shown. The shading depicts the solvent accessibility of each residue, where white and black represent the most and least accessible regions, respectively. Residues −5 to 8 are not included because of the unavailability of sufficient assignments in this region of the protein.

already described.[16] At the end of this process, no unassigned NOESY cross peaks were detectable in the spectrum.

Calibration of NOEs. The best calibration of observed intensities was found to be inversely proportional to the sixth power of the proton−proton distances for calibration classes 3 (medium range NOEs) and 4 (long range backbone), to the fifth power for calibration classes 1 (intraresidue, except HN, Hα, and Hβ) and 2 (sequential and intraresidue HN, Hα, and Hβ), and to the second power for class 5 (long range). Deviations from the theoretical sixth-power dependence can be ascribed to dynamic effects.[40] The present result is consistent with quite a high level of protein mobility. As expected, the intensities of the long range side-chain NOEs are affected the most by this characteristic.

Family of Structures. The final set of constraints, consisting of 1158 experimental NOEs, 203 pseudocontact shifts, and 50 backbone dihedral angles, was used to generate a family of structures by standard PARAMAGNETIC-DYANA calculations starting from random conformations. Of the 838 meaningful NOE constraints, 165 are intraresidue, 239 are sequential, 191 are medium range, and 243 are long range connectivities. The breakdown of experimental constraints per residue is summarized in Figure 5. The family of structures generated in this way was refined by restrained energy minimization (REM) calculations.

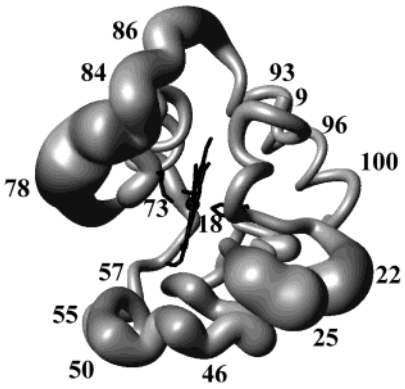

Figure 6. Backbone of the family of 20 REM structures shown as a tube of variable radius. The radius is proportional to the RMSD of each residue. The figure is generated with the program MOLMOL.[51] The heme and the two axial ligands are shown in black.

The target function of the resulting family is 2.9 ± 0.2 Å^2, which compares well with that reported for the solution structure of wild-type cyt *c* (3.01 ± 0.08 Å^2).[15] The NOE constraint contribution to the total target function is 1.3 ± 0.2 Å^2. These figures indicate that there is satisfactory agreement between the resulting structure and the imposed constraints and also among sets of constraints which are different in nature. The latter is an important requirement to gain confidence in the accuracy of the calculated structure. The backbone RMSD value, calculated with respect to the average structure and superimposing residues 9−102, is 1.5 ± 0.2 Å. The present family of structures provides a clear picture of the folding, and the analysis of the RMSD per residue allows one to learn which regions are well-defined and which are not. The overall shape of the molecule as well as its secondary structure and the RMSD per residue are depicted in Figures 5 and 6. Valuable structural information on the alkaline form of ferricytochrome *c* can be gained by the analysis of this family of structures. In Figure 7, the average energy-minimized structure is compared with that of the native protein. Native ferricytochrome *c* is globular and consists of five helices, H1, H2, H3, H4, and H5, which span the regions 6−13, 50−55, 61−69, 70−75, and 89−103, respectively. The structure of alkaline ferricytochrome *c* is also characterized by a globular fold with remarkably similar protein dimensions. The two longest helices, H1 and H5, maintain (at least for the assigned residues) native local conformations, their reciprocal arrangements, and their positions with respect to the heme moiety. The 20s and 40s loops are among the regions that differ the most from the native structure. However, these regions are poorly defined in both the native protein and the alkaline form, so that the observed differences are essentially within the experimental uncertainties of the structures. Residues 51−55 fold into a helix that is less well-defined than H2 in the native protein. In addition, the large structural changes that occur among residues 70−81 to accommodate the ligand exchange affect the position of residues of H4 in the native protein. Despite the high RMSD values in this region, NOE peaks unique to the alkaline form corroborate the main conformational differences from the native structure. These NOEs define the proximity of Ile75 to residues

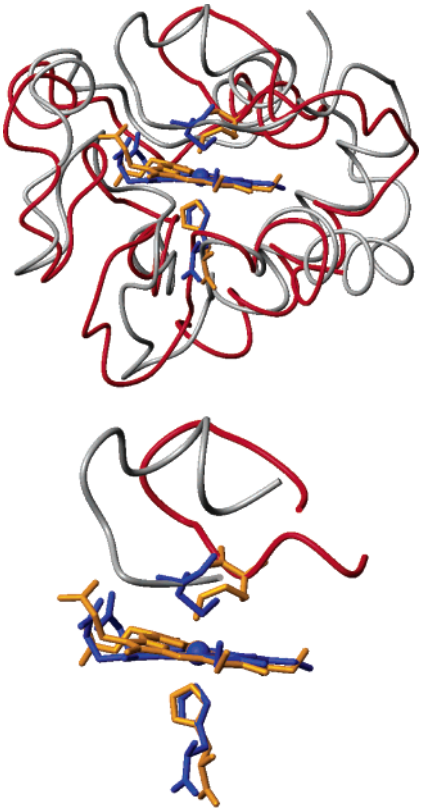

Figure 7. The average solution structure of the K79A variant (represented in red) is compared to the average solution structure of the native protein (represented in gray) in terms of backbone fold (top). The heme moiety and the axial ligands are shown in orange for the K79A variant and in blue for the native cytochrome *c*. The heme core is shown in greater detail (bottom) using the same color scheme. These figures were generated with the program MOLMOL.[51]

55, 57−60, 62−64, and 73. They also constitute unequivocal proof of the altered conformation of the loop that is independent of considerations concerning the nature of the new axial ligand and, consequently, of the distance constraints imposed between Lys73 and the heme iron atom. Finally, H5 maintains its native position despite the structural changes of loop 70−80. Although an increase in mobility seems a general feature of the alkaline conformer, the effect is particularly evident in the 80s loop. The obtained structure shows that, at high pH, the latter loop has no specific interactions to the rest of the protein, the coordination bond between the iron and Lys73 being the only anchoring point able to maintain the compactness of the distal site of the protein. Consistent with this picture, *Bacillus pasteurii* cytochrome *c*, which has no lysines in the corresponding distal loop, becomes completely unfolded upon breaking of the methionine−iron bond.[55]

The side-chain NHs of Glu16, Asn31, Asn52, Trp59, and Asn63 remain detectable at pH 11.1, suggesting that these residues are involved in strong H-bond interactions. However, the acceptors of these H-bonds could not be identified because of the low resolution of these side chains.

Further analysis of the structures also shows that, of the residues relevant to the Ramachandran plot (i.e., nonglycine, nonproline, and nonterminal residues), 48.2% fall in the most favored regions, 41.0% in additional allowed regions, 7.2% in generously allowed regions, and 3.6% in disallowed regions. The corresponding numbers for the energy minimized average structure are 50.0%, 35.6%, 12.2%, and 2.2%, respectively. It is noteworthy that 7 out of 11 residues falling in generously allowed regions and the two falling in the disallowed region are not assigned. The G-factor is −0.80, and the H-bond energy is 0.9 kcal/mol. The structure presents zero bad contacts. All these parameters indicate a satisfactory quality for a structure with the present resolution.

Role of the Distal Loop. The movement of the distal loop in the present structure provides the key to interpret some important experimental observations about cytochrome *c* chemistry, while the observed protein flexibility could be relevant for the proposed role of this protein form in protein recognition.

A. Redox Potential of the Alkaline Form. From comparison of the native and alkaline ferricytochrome structures (Figure 7), it is evident that the distal loop region moves away from the heme moiety at alkaline pH. Interestingly, the conformational rearrangement in this region of the protein appears to open a channel to the heme pocket. Comparison of the solvent accessibility of the heme in the energy-minimized, averaged structures of the native and alkaline conformers (evaluated with the program MOLMOL) suggests that the solvent exposure of the heme (when considering the iron ion and the carbon and nitrogen atoms which form the π-conjugate porphyrin system) increases by nearly 20%. Increased exposure of the heme group to the solvent is consistent with the nearly 0.5 V drop in the protein midpoint reduction potential.[27,56,57]

B. Redox Dependent Stability of Cytochrome *c*. That only the oxidized form of the protein undergoes an alkaline transition is generally attributed to the lower stability of the Met80−Fe(III) bond relative to that of Met80−Fe(II).[52,58] As a result, the ferricytochrome exhibits a more flexible structure than the ferrous form of the protein.[14−17,52,59−64] The present results indicate that the regions that display major structural changes due to the alkaline transition correspond to those that exhibit increased conformational dynamics upon oxidation,[64] thereby confirming the relationship between these phenomena.[56,64] The same protein region is involved in the conformational transition occurring upon exogenous ligand binding.[65] In light of the different NOE patterns (oxidized versus reduced forms) involving amino acids of helix H2 on one side and of helix H4 and the 80s loop on the other, we propose that upon oxidation the interaction between these two regions of the protein relax, make the polypeptide more mobile, and destabilize the native conformation of the 80s loop. At high pH values, this effect allows a deprotonated lysine to replace Met80 as a heme ligand. The

(55) Bartalesi, I.; Bertini, I.; Ghosh, K.; Rosato, A.; Turano, P. *J. Mol. Biol.* **2002**, *321*, 693−701.
(56) Tezcan, F. A.; Winkler, J. R.; Gray, H. B. *J. Am. Chem. Soc.* **1998**, *120*, 13383−13388.
(57) Battistuzzi, G.; Borsari, M.; Cowan, J. A.; Ranieri, G. A.; Sola, M. *J. Am. Chem. Soc.* **2002**, *124*, 5315−5324.
(58) Chin, J. K.; Jimenez, R.; Romesberg, F. E. *J. Am. Chem. Soc.* **2002**, *124*, 1846−1847.
(59) Englander, S. W.; Kallenbach, N. R. *Q. Rev. Biophys.* **1983**, *16*, 521−655.
(60) Englander, S. W. *Science* **1992**, *256*, 1684−1687.
(61) Bai, Y. W.; Sosnick, T. R.; Mayne, L.; Englander, S. W. *Science* **1995**, *269*, 192−197.
(62) Milne, J. S.; Mayne, L.; Roder, H.; Wand, A. J.; Englander, S. W. *Protein Sci.* **1998**, *7*, 739−745.
(63) Baxter, S. M.; Fetrow, J. S. *Biochemistry* **1999**, *38*, 4493−4503.
(64) Barker, P. B.; Bertini, I.; Del Conte, R.; Ferguson, S. J.; Hajieva, P.; Tomlinson, E. J.; Turano, P.; Viezzoli, M. S. *Eur. J. Biochem.* **2001**, *268*, 4468−4476.
(65) Yao, Y.; Quian, C.; Ye, K.; Wang, J.; Bai, Z.; Tang, W. *JBIC, J. Biol. Inorg. Chem.* **2002**, *7*, 539−547.

Table 2. Parameters Characterizing the Magnetic Susceptibility Tensor in the Alkaline Form of Cytochrome *c*[a]

	alkaline K79A yeast cytochrome *c*	wild-type yeast cytochrome *c*[15] [b]	M80A yeast cytochrome *c*-CN$^-$ [46] [b]
$\Delta\chi_{ax}$ ($/10^{-32}$ m^3)	2.68 ± 0.16	2.36 ± 0.09	3.05 ± 0.10
$\Delta\chi_{rh}$ ($/10^{-32}$ m^3)	-0.48 ± 0.17	-1.20 ± 0.13	-0.47 ± 0.12
deviation of the *z* axis from the perpendicular to the heme plane (deg)	12 ± 2	14 ± 2	2 ± 2
deviation of the *x* axis from the $\alpha-\gamma$ meso direction (deg)	85 ± 11	52 ± 10	98 ± 9

[a] These parameters are compared to those of the native protein and the cyanide adduct of the M80A variant. [b] The five tensor parameters and their errors have been recalculated here with the Monte Carlo approach and therefore could be slightly different with respect to those reported in the cited references.

change in axial ligand is thus closely linked to flexibility and consequent structural destabilization of the native fold, consistent with the fact that the pK_a of the transition to the alkaline form is greatly reduced at high temperatures and/or in the presence of chemical denaturants.

Magnetic Susceptibility Tensor. The magnetic susceptibility tensor parameters were calculated for the family of refined structures, and the resulting values are reported in Table 2 along with the tensor parameters of native ferricytochrome *c* and the cyanide adduct of the M80A variant. The calculated axial anisotropy thus appears to be slightly higher and the rhombic component, lower than those of the native protein[15] but closer to those calculated for the CN$^-$ adduct of the M80A variant.[46] The rhombic-axis direction in the alkaline form of the K79A ferricytochrome is clearly closer to that of the CN$^-$ adduct of the M80A variant. Additional experimental evidence for the orientation of the magnetic susceptibility tensor can be obtained from the chemical shifts of the four heme methyl groups. For ferriheme proteins, the chemical shifts of these protons are related to the orientation of the axial ligands through the following heuristic relation:[66]

$$\delta_i = [a \sin^2(\vartheta_i - \phi) + b \cos^2(\vartheta_i + \phi) + c] \qquad (2)$$

where ϑ_i is the angle between the metal−methyl-3 and the metal−pyrrole II directions, and the coefficients *a*, *b*, and *c* are factors determined for heme proteins for which both the experimental shifts of the heme methyl groups and the orientation of the ligands are known. In the case of heme proteins where one axial ligand is a His residue and the other ligand does not contribute to the rhombicity of the magnetic tensor (e.g., CN$^-$), $a = 18.4 \pm 2.4$, $b = -0.8 \pm 2.0$, $c = 6.1 \pm 1.9$ ppm. In systems with this axial coordination, the *x*-axis of the magnetic susceptibility tensor forms an angle equal to $-\phi$ with the metal−pyrrole II direction. With the previous values for the parameters *a*, *b*, and *c* and the experimental shifts, an angle ϕ of 60° is obtained. This value and the corresponding orientation of the tensor are comparable to those obtained for the cyanide adduct of ferricytochrome *c*. These results are consistent with the presence of a His ligand with the plane of the imidazole group approximately aligned with the $\alpha-\gamma$ *meso* direction of the heme. This situation is similar to that encountered for the protein in the native state and, thus, with an *x*-tensor axis aligned in the direction of the other pair of *meso* protons.

(66) Bertini, I.; Luchinat, C.; Parigi, G.; Walker, F. A. *JBIC, J. Biol. Inorg. Chem.* **1999**, *4*, 515−519.

Conclusions

We report the first structural characterization of an alkaline form of mitochondrial ferricytochrome *c*. At pH 11.1, the sixth heme ligand in the K79A variant of oxidized *S. cerevisiae* cytochrome *c* is Lys73 (Lys73 NMR signals were observed for the first time).

Because of the high pH required for these experiments, the structural determination was not straightforward. Nevertheless, 94 backbone NHs were detected in HSQC experiments, although dipolar connectivities were not observed for many of them and, therefore, they could not be assigned because of the high mobility of the corresponding backbone area. The alkaline form of cyt *c* does possess higher flexibility than that of the native protein, as indicated by heteronuclear NOE data. As a consequence, the resulting family of structures is characterized by a lower precision of the coordinates with respect to those of similarly sized proteins determined under native conditions. Selected protein regions, with mainly helical elements, are quite well-defined in the current structure and are similar to the same regions in the native form. Only small changes are observed for the polypeptide surrounding the proximal histidine ligand. A few important NOEs confirm that substantial rearrangement in the loop containing Lys73 is associated with the alkaline conformational transition. The resulting family of structures is of good quality based on Ramachandran plot parameters and the agreement among experimental constraints.

From a methodological point of view, our approach contains hints for the structural characterization of highly flexible forms of globular paramagnetic metalloproteins.

The magnetic susceptibility tensors calculated for the family of structures indicate that the electronic structure of the K79A ferriheme at high pH resembles that of M80A CN-ferricytochrome *c*. This result is in agreement with axial coordination by Lys73 because such ligation would not contribute to the rhombicity of the magnetic anisotropy tensor and lysine ligation is supported by other spectroscopic data.[23] At the same time, the obtainment of a univocally determined set of tensor parameters is an indication of a well-defined structure.

The structure of the alkaline conformer resulting from this work is a general model for compact intermediates of cyt *c* that are presumably involved in unfolding processes at high temperatures or induced by high concentrations of denaturants. One of the most interesting features of the fold of the alkaline form is that the rearrangement of the distal loop increases the solvent accessibility of the heme. It has been estimated from GuHCl-induced unfolding studies that ferrocytochrome *c* is about 10 kcal mol^{-1} more stable toward unfolding than ferricytochrome

c,[67,68] a finding that is attributable to stabilization of the ferroheme by hydrophobic encapsulation and enhanced iron−methionine bonding.[56] A 10 kcal mol^{-1} difference in conformational energy between native and alkaline forms estimated from reduction potentials also has been ascribed to differences in axial ligation and heme solvent exposure.[27] Using model systems, we have estimated that the former effect represents roughly 30% of the total stability difference.[56] Our work is the first to establish unequivocally that greatly increased heme solvent exposure is a major contribution to the 10 kcal mol^{-1} destabilization of Lys73 ligated cytochrome *c*.

(67) Pascher, T.; Chesick, J. P.; Winkler, J. R.; Gray, H. B. *Science* **1996**, *271*, 1558−1560.
(68) Mines, G. A.; Pascher, T.; Lee, S. C.; Winkler, J. R.; Gray, H. B. *Chem. Biol.* **1996**, *3*, 491−497.

Acknowledgment. We thank the MIUR COFIN2001 and EU TMR Network (FMRX-CT98-0218) (I.B.), Italian CNR (Progetto Finalizzato Biotecnologie 01.00359.PF49) (P.T.), Operating Grant MT-14021 from the Canadian Institutes of Health Research and a Canada Research Chair (A.G.M.), and the National Science Foundation (H.B.G.).

Supporting Information Available: Tabulated NMR chemical shifts and pseudocontact shifts of the alkaline form of *S. cerevisiae* cytochrome *c*; the experimental NOESY cross peak intensities; and the corresponding upper distance limits used in the structure calculations. This material is available free of charge via the Internet at http://pubs.acs.org.

JA027180S